Demographic analysis for silky shark (*Carcharhinus falciformis*) in the Indian Ocean

Jizhang Zhu, Zhe geng, Yanan Li, Jiangfeng Zhu, Xuefang Wang

College Marine Living Resource Sciences and Management, Shanghai Ocean University

Summary

This study investigated the key parameters for the population dynamic of the silky shark (*Carcharhinus falciformis*) in the Indian Ocean through demographic analysis. To evaluate the impact of uncertainties in survival rates on demographic parameter estimates, we developed six scenarios based on growth parameters and age-at-maturity data specific to the Indian Ocean. These scenarios accounted for reproductive cycles of 1-2 years and 1-3 years, respectively. Through 10000 Monte Carlo simulations, we estimated the intrinsic rate of population increase (γ), net reproductive rate (R_0), generation time (G), population doubling time (t_{x2}), and steepness (h). The results indicated that the mean intrinsic growth rate varied between 0.072 and 0.136 across different scenarios. The mean R_0 ranged from 3.18 to 5.59, the mean generation time ranged from 10.7 to 17.4 years, the mean t_{x2} ranged from 5.13 to 9.92 years, and the mean h ranged from 0.291 to 0.506. Scenarios with a lower age at maturity and shorter reproductive cycles showed higher growth rates and shorter doubling times, indicating more favorable population dynamics. However, uncertainties in life history data and model estimations influenced these results, emphasizing the importance of accounting for multiple scenarios and uncertainties when developing population management and conservation strategies.

1 Introduction

Carcharhinus falciformis (*Carcharhiniformes*, *Carcharhinidae*, *Carcharhinus*), known as the silky shark, is a highly migratory species, the silky shark is widely distributed in the upper layers of tropical and subtropical oceans, ranging from 42°N to 43°S*(Compagno, 2001; Strasburg, 1958)*, with a preference for water temperatures exceeding 23°C *(Varghese et al., 2016)*. This makes it one of the most widely distributed shark species globally. In the western Indian Ocean, the silky shark is commonly found along the continental shelf edges and near islands, extending from the Red Sea in the north to the coastal waters of Mozambique and the Maldives in the south. Silky sharks exhibit late maturity and longevity, reaching a maximum length of up to 350cm *(Compagno, 2001)*. The longevity for males is 28.6 years, while females can live up to 35.8 years *(Joung et al., 2008)*. Due to the silky shark's slow growth and low reproductive capacity, it is particularly vulnerable to overfishing *(Cortés, 2000; Joung*

et al., 2008). The silky shark is targeted by some semi-industrial fisheries, artisanal fisheries, and recreational fisheries *(Burns et al., 2023)*. It is also a major bycatch species in tuna longline, gillnet, and purse seine fisheries. Some studies indicate that the silky shark is currently experiencing significant fishing pressure *(Filmalter et al., 2013)*.

Indian Ocean Tuna Commission Scientific Committee recommends utilizing various assessment methods, including biomass dynamics and age-structured models, to evaluate the stock status of the Indian Ocean Silky Shark and provide better management advice. While biomass dynamics models require external estimates for γ, age-structured models depend on h values, which are challenging to determine.

Research has suggested that the reproductive cycle of the silky shark is biennial, as evidenced by the absence of developing ova in pregnant females -- a feature typical of species with a two-year reproductive cycle *(Galván-Tirado et al., 2015; Hoyos-Padilla et al., 2012)*. Typically, the reproductive cycle of the silky shark ranges from 1 to 2 years, although it can extend up to 3 years due to regional variations, maternal health, and environmental factors *(Branstetter, 1987; Joung et al., 2008)*. The reproductive cycle significantly influences life history parameters such as the intrinsic growth rate of the population *(Cortés, 2000; Joung et al., 2008; Smith et al., 1998)*. *Tsai et al. (2018)* have already considered this reproductive cycle issue in their research *(Tsai et al., 2019)*. This study, however, takes into account that no seasonal reproductive activity of the silky shark has been observed in the Indian Ocean *(Hall et al., 2012)*, suggesting a potentially broader variability in reproductive cycles.

Given the current lack of information and uncertainty regarding the population status, this study has collected relevant biological parameters for the silky shark in the Indian Ocean and utilized Monte Carlo simulations to account for the uncertainties in these parameters. To more comprehensively assess the potential reproductive cycles, this study proposes that the reproductive cycle of the silky shark may range between one to two years or one to three years, influenced by factors such as post-partum rest periods, individual migratory behavior, and mating success rates. Additionally, research by various scholars suggests that there may be variability in the age of sexual maturity for the silky shark *(Hall et al., 2012; Varghese et al., 2016)*. This study simulates the impacts of these different scenarios on key parameters through various scenarios and employs Leslie matrices for analysis. By constructing Leslie matrices reflecting the survival and reproductive rates among different age groups of the silky shark, we are able to effectively predict population dynamics. The results of this study will provide important insights for developing scientific fisheries management strategies and resource protection measures, thereby contributing to the sustainable utilization and effective management of the silky shark population.

2 Materials and methods

2.1 Demographic method

This study employed a two-sex Leslie population projection matrix *(Caswell, 2006; Geng et al.,, 2021; Yokoi et al., 2017)* to represent the population structure of the Indian Ocean Silky Shark:

$$N_{t+1} = \mathbf{M}N_t \tag{1}$$

the matrix **M** is a Leslie population projection matrix, where $\boldsymbol{N}_t$ represents the vector of numbers at each age in year t.

$$\mathbf{M} = \begin{bmatrix} F_{0,m} & F_{1,m} & \dots & F_{max-1,m} & F_{0,f} & F_{1,f} & \dots & F_{max-1,f} & 0 \\ pS_{0,m} & 0 & \dots & 0 & 0 & 0 & \dots & 0 & 0 \\ 0 & S_{1,m} & \dots & 0 & 0 & 0 & \dots & 0 & 0 \\ \vdots & \vdots & \ddots & \vdots & \vdots & \vdots & \vdots & \vdots & \vdots \\ 0 & 0 & \dots & S_{max-1,m} & 0 & 0 & \dots & 0 & 0 \\ (1-p)S_{0,f} & 0 & \dots & 0 & 0 & 0 & \dots & 0 & 0 \\ 0 & 0 & \dots & 0 & 0 & S_{1,f} & \dots & 0 & 0 \\ \vdots & \vdots & \dots & \vdots & \vdots & \vdots & \ddots & \vdots & \vdots \\ 0 & 0 & \dots & 0 & 0 & 0 & \dots & S_{max-1,f} & 0 \end{bmatrix} \tag{2}$$

Where S_x is the annual natural survivorship of age x for male(m) and female(f). The F_x elements represent the age-specific per-capita fecundity rates. The p is the sex ratio in out study, and equal to 0.5 for the Indian Ocean silky shark. A birth-pulse population and a post-breeding census were assumed *(Caswell, 2006)*. Accordingly, the first age class (age 0) is represented by the newborn pups, and the fecundity (F_x) terms include the probability that a pregnant female survives and delivers pups at the end of the year.

According to matrix algebra $\mathbf{M}N_t = \lambda N_t$, where λ is the eigenvalue of matrix **M**. Therefore, λ is the finite rate of population increase, and $\boldsymbol{\gamma} = \ln \lambda$ is the intrinsic rate of population increase. The value of λ is determined by finding the dominant eigenvalue of **M** *(Simon et al., 2012)*. The underlying assumption of the matrix model (Equations and 2) is that the population will grow exponentially and reach a stable age distribution (*sad*) *(Caswell, 2006)*. Therefore, to estimate $\boldsymbol{\gamma}$ and its uncertainty, several biological parameters (e.g., growth and longevity) and their uncertainty need to be estimated, as described in the following sections.

The Beverton Holt (B-H) and Ricker models are two widely used stock-recruitment relationships in stock assessment. The B-H model operates under the assumption of density-dependent mortality rather than abundance-dependent mortality. Following the method of *Myers et al. (1999)*, we calculated the *h* of the B-H stock-recruitment model using parameters from the demographic analysis:

$$\hat{\alpha} = \alpha \cdot SPR_{F=0} \quad (3)$$

$$h = \frac{\hat{\alpha}}{4+\hat{\alpha}} \quad (4)$$

where $\hat{\alpha}$ represents the number of spawners produced per spawner over its longevity, $SPR_{F=0}$ is the spawning biomass per recruit at an unfished equilibrium population size(obtained from R_0), and α is the slope of the population at the origin(extremely low population size). In the context of the Beverton-Holt (B-H) stock-recruitment curve, α also refer to the maximum density-independent survival rate, which can be estimated from the number of recruits and spawners (or pups). *Brooks et al. (2010)* demonstrated that for sharks where eggs could be counted, α is equivalent to first-year (pups) survival. For more theoretical and analytical details on the estimation of *h*, refer to the studies by *Myers et al. (1999)* and *Brooks et al. (2010)*. All demographic and simulation analyses in this study were conducted using the R language for statistical computing.

2.2 Life-history parameters and uncertainty

Growth and longevity

There is a notable paucity of research regarding the age and growth of silky sharks in the Indian Ocean (Table 1). Within the broader Indian Ocean, *Hall et al. (2012)* and *Varghese et al. (2016)* are the primary references for growth parameter studies on silky sharks. *Hall et al. (2012)* analyzed 78 male and 90 female specimens, while *Varghese et al. (2016)* conducted a complementary study. The former employed vertebral centrum sections for age estimation, whereas the latter utilized length-frequency analysis.

This study used 159 silky sharks captured by Chinese longline observers in the western Indian Ocean between 2010 and 2020 as research samples (Figure 1). For these samples, fork length and sexual maturity status were recorded. The von Bertalanffy growth parameters were estimated using the ELEFAN I method based on length-frequency data *(Varghese et al., 2016)*. The results of the growth equations are presented in Table 1.

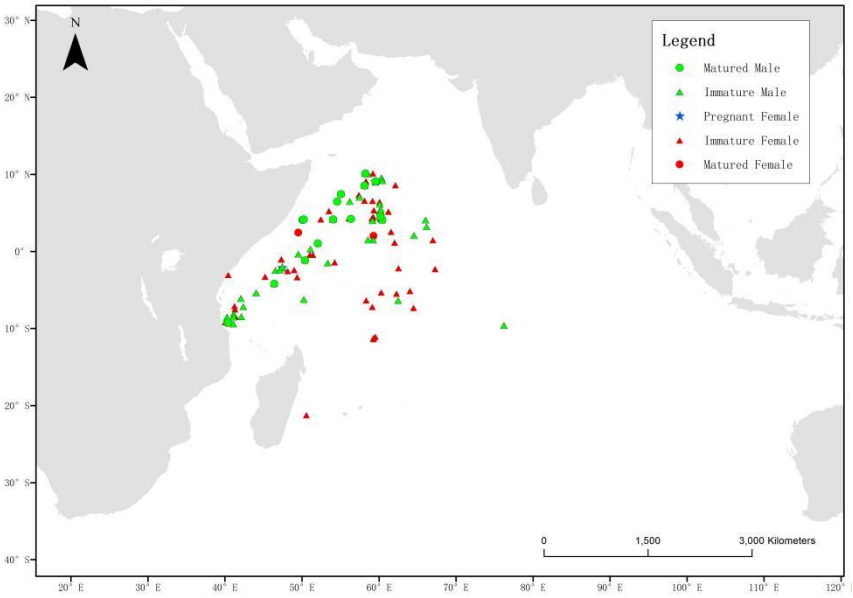

Figure1. The capture location of the silky shark used in this study

Varghese et al. (2016) argued that age-length data provides a more accurate estimation of growth parameters when feasible. Currently, there is a lack of research assessing the precision of growth equations derived from the length-frequency method for silky sharks.

Table.1 Comparison of growth parameters of the growth equation of silky sharks reported by various studies.

Author	**Sampling area**	**Method**	**Gender**	L_{inf}**(cm)**	K**(year^{-1})**	t_0**(year)**
(Branstetter, 1987)	Northwestern Gulf of Mexico	VCS	Combine	291	0.153	-2.2
(Bonfil, 1997)	Maxican Caribbean	VCS		311	0.101	-2.72
(Oshitani, Nakano, & Tanaka, 2003)	Pacific Ocean	VCS		287.7	0.148	-1.76
(Joung et al., 2008)	Northwest Pacific	VCS		332	0.084	-2.76
(Sánchez‐de Ita, Quiñónez‐Velázquez, Galván‐Magaña, Bocanegra‐Castillo, & Félix‐Uraga, 2011)	West coast of Baja California Sur	VCS		240	0.14	-2.98
(Hall et al., 2012)	Off Indonesia	VCS	Combine	299.4	0.066	
			M	277.3	0.079	
			F	320.4	0.057	

(Varghese et al., 2016)	Eastern Arabian Sea	LFA	Combine	309.8	0.1	-2.4
(Grant et al., 2018)	Central West Pacific	VCS		268.3	0.14	
This study	West Indian Ocean	LFA	Combine	328.6	0.08	-0.51

Note: VCS, Vertebral Centrum Sections for age reading; LFA, Length Frequency Analysis.

In the study by *Joung et al. (2008)*, the maximum observed age for silky shark in the Northwest Pacific Ocean was 22 years, while the theoretical maximum age was estimated to be 35 years. Specifically, the estimated longevity is 28 years for males and 35 years for females. *Grant et al. (2018)* reported that the maximum age of silky sharks caught in the Western and Central Pacific was 28 years. *Hall et al.(2012)* reported maximum ages of 20 years for males and 19 years for females in their samples. According to *Tsai et al. (2018)*, the most reliable approach for estimating longevity involves using the observed maximum age as a lower limit and the theoretical maximum age as an upper limit for parameter inputs. Consequently, this study defines the longevity range for silky sharks between 25 and 35 years, applying a uniform distribution across this range to randomly generate longevity values for each sample.

Maturity and fecundity

Table 2 provides a summary of studies on the reproductive biology of silky sharks. This study estimates the size at 50% sexual maturity for silky sharks based on observer records, with males reaching this maturity at a fork length of 157.58 cm (n=65) and females at 200.76 cm (n=56) (Figure 2).

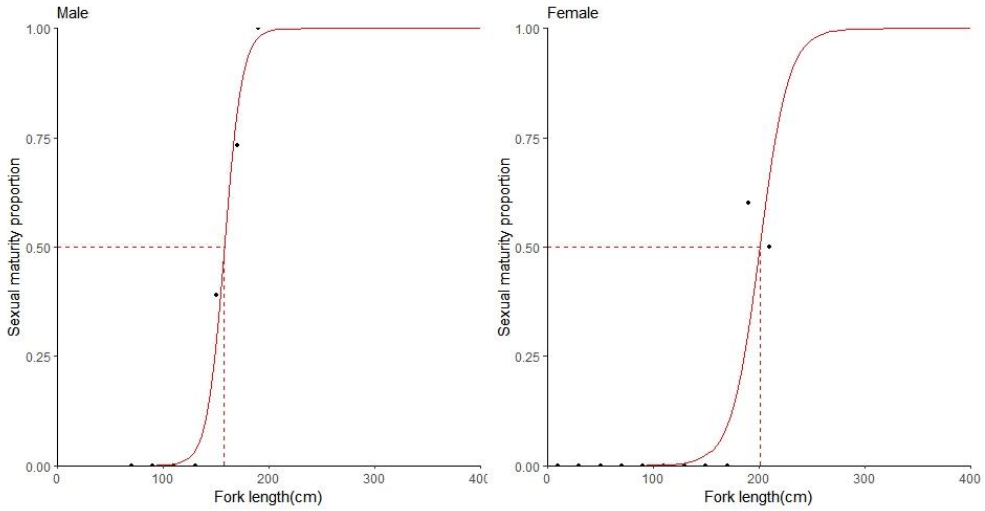

Figure.2 The relationship between sexual maturity proportion and fork length (cm) in male and female silky sharks. The red curve represents the logistic curve.

Silky shark exhibits placental viviparity, a reproductive strategy that enhances the size of neonates, thereby improving their environmental adaptability and increasing juvenile survival rates *(Galván-Tirado et al., 2015)*. Research by *Grant et al. (2020)* and

Oshitani et al. (2003) indicates that the reproductive capacity of the silky shark does not increase with the maternal s length, suggesting no significant correlation between body length and fecundity. Furthermore, studies have shown that the gestation period for silky sharks is approximately 11-12 months *(Hoyos-Padilla et al., 2012)*, with litter sizes ranging from 2 to 14 embryos and an average of 7.2 embryos per litter, maintaining a 1:1 sex ratio *(Alejo-Plata et al., 2016; Hall et al., 2012; Hazin et al., 2007; Joung et al., 2008)*.

Several scholars propose that the reproductive cycle of the silky shark is biennial, supported by the absence of developing ova in pregnant females—a hallmark of species with a two-year reproductive cycle *(Galván-Tirado et al., 2015; Hoyos-Padilla et al., 2012)*. Some studies have documented the seasonal reproductive activity*(Bonfil, 1997; Galván-Tirado et al., 2015)*. *Bonfil (1997)* reported a 12-month gestation period in the Gulf of Mexico, with a fixed parturition season from May to June. *Oshitani et al.(2003)* analyzed the maturity of embryos in pregnant females across different quarters and concluded that the birthing season for silky sharks in the tropical Pacific Ocean spans from May to July. *Alejo-Plata et al. (2016)* found that silky sharks give birth throughout the year, with a peak birth rate from May to October. Conversely, other researchers argue that there are no significant seasonal differences in the reproduction of silky sharks in the Indian Ocean *(Hall et al., 2012)* and the Pacific Ocean *(Galván-Tirado et al., 2015; Hoyos-Padilla et al., 2012; Joung et al., 2008)*. *Hazin et al. (2017)* noted that silky sharks near the equator do not display a distinct seasonal pregnancy cycle. This discrepancy suggests that further research is needed to clarify the reproductive patterns of silky sharks.

Accordingly, this study models the fecundity of silky sharks using a uniform distribution with a mean of 7.2 and a range of 2 to 14 embryos, under the assumption that fecundity is independent of body length and age. To further simulate the effects of varying reproductive cycles on population dynamics, we assume reproductive cycles of 1-2 years and 1-3 years, incorporating random values within these ranges in the model for simulation analysis. This approach is grounded in *Tsai et al. (2019)* study on the reproductive cycles of one and two years, while also accounting for potential natural variability in reproductive cycles to enhance the model's scientific validity and predictive accuracy.

Table.2 Comparison of length at maturity (L_T50), age at maturity (A50), length at birth (L_b) and brood size of silky sharks reported by various studies.

Area	**L_T50(cm)**		**A50(year)**		**L_b(cm)**	**Litter size**	**Reference**
	Males	Females	Males	Females			
Pacific ocean							
Central Pacific Ocean		202—208					*(Strasburg, 1958)*
Tasman Sea, Australia	214	202—208					*Stevens (1984a)*
Northern Australia	210	215					*(females)(Stevens & McLoughlin, 1991)*
Eastern Pacific	180	180			70		*Cadena-Cardenas(2001)*
Southern Mexican Pacific	180	190			60—69	2—14	*(Galván-Tirado et al., 2015)*
Tropical Pacific Ocean	200—206	186	5—6	6—7	65—81	1—16	*(Oshitani et al., 2003)*
Northwest Pacific	212.5	210—220	9.3	9.2—10.2	63.5—75.5	8—10	*(Joung et al., 2008)*
Central west Pacific	183	204	11.6	14	66—71	9—12	*(Grant et al., 2018)*
Indian ocean							
Off Madagascar	240	248—269					*Fourmanoir (1961)*
Southeastern Africa	240	248—260			78—87		*Bass(1973)*
Maldives					56—63		*(Anderson, Ahmed, & Ministry of Fisheries, 1993)*
Aldabra Atoll	239	216					*(Stevens, 1984)*
Eastern Arabian Sea	218.98	227.76	9.87	10.89	65.1—67	3—13	*(Varghese et al., 2016)*
Off Indonesia	207.6	215.6	13—14	14—16	81.1	2—14	*(Hall et al., 2012)*
Atlantic Ocean							
Florida coast							*Springer(1960)*

Gulf of Guinea		238					*(Bane, 1966)*
Campeche Bank	225	232—246			76		*(Bonfil, 2008)*
Unspecified	220	250					*Cadenat and Blanche(1981)*
West coast of Mexico	182	180			80	2—9	*(Hoyos-Padilla et al., 2012)*
Northern Gulf of Mexico	210—220	225	6—7	7—9	76	2—12	*(Branstetter, 1987)*
Gulf of Mexico	225	232—245	10+	12+			*(Bonfil, 1997)*

Note: L_T50 is the length at which 50% of individuals reach sexual maturity, A50 is the age at which 50% of individuals reach sexual maturity, L_b is the length at birth, and Brood size refers to the number of offspring.

Natural mortality and survival rate

Age-specific survival rate (S_t) is defined as:

$$S_t = \mathrm{e}^{-M_t} \quad (5)$$

where M_t is the (instantaneous) natural morality for age t. Natural mortality is notoriously challenging to estimate, making it a significant source of uncertainty in population dynamics modeling. Consequently, we employed three empirical methods to estimate *M*:

(1) The *Then et al. (2015)* method, which updated *Hoenig's (1983)* method, i.e.,

$$M = 4.899 {t_{max}}^{-0.916};$$

(2) The *Jensen (1996)* method, which estimates *M* based on the age-at-maturity(t_{mat}; the age-at-delivery less gestation period), i.e.,

$$M = \frac{1.65}{t_{mat}};$$

(3) The method by *Chen and Watanabe's (1989)*, which estimates *M* through a relationship with growth parameters (including their associated uncertainties) and age at maturity.

Methods (1) and (2) yield age-independent estimates of *M*, whereas Method (3) provides age-specific estimates of *M*.

Accounting for uncertainty

The impact of uncertainty in life-history parameters was addressed through Monte Carlo simulations. This process involved estimating the distribution of natural mortality *M* whether age-invariant or age-specific, by sampling from the distributions of life-history parameters (e.g. L_{inf}, L_0, age-at-maturity, longevity, etc.) . Each estimate of *M* was derived from a single sampling instance. In total, 4,000 vectors of M-at-age, collectively referred to as "ALL methods," were generated, with 1,000 vectors for each estimation method.

For estimating annual survival rates, this study utilized a triangular distribution (probability density function, pdf), following the approach outlined by *Caswell (2006)*. The triangular distribution is well-suited for representing uncertainty in life-history parameters prior to performing stochastic demographic analyses, as it facilitates the specification of lower and upper bounds along with a most likely value within this range *(Aires-da-Silva & Gallucci, 2007; Cortés, 2002, 2008)*. Although log-normal distributions are sometimes used as an alternative, they generally produce similar results, particularly in terms of central tendency measures *(Aires-da-Silva & Gallucci,*

2007; Cortés, 2002). Consequently, this study exclusively employed the triangular distribution for modeling annual survival rates.

For each age, the minimum and maximum survival rates derived from the 4,000 estimates of *M* were used as the bounds of the triangular distributions, with the mean value representing the most likely estimate. These probability density functions were then applied as survival rates in the demographic analysis.

In this study, the reproductive cycle of the silky shark is modeled to range between one to two years or one to three years, taking into account factors such as post-partum rest periods, individual migratory behavior, and mating success rates. For the recruitment pattern one(RP1) , a lognormal probability density function will be used to randomly generate reproductive cycle values within this range for each iteration (Figure 3a). For the recruitment pattern two(RP2), a normal probability density function will be employed to generate reproductive cycle values within the specified range for each iteration (Figure 3b).

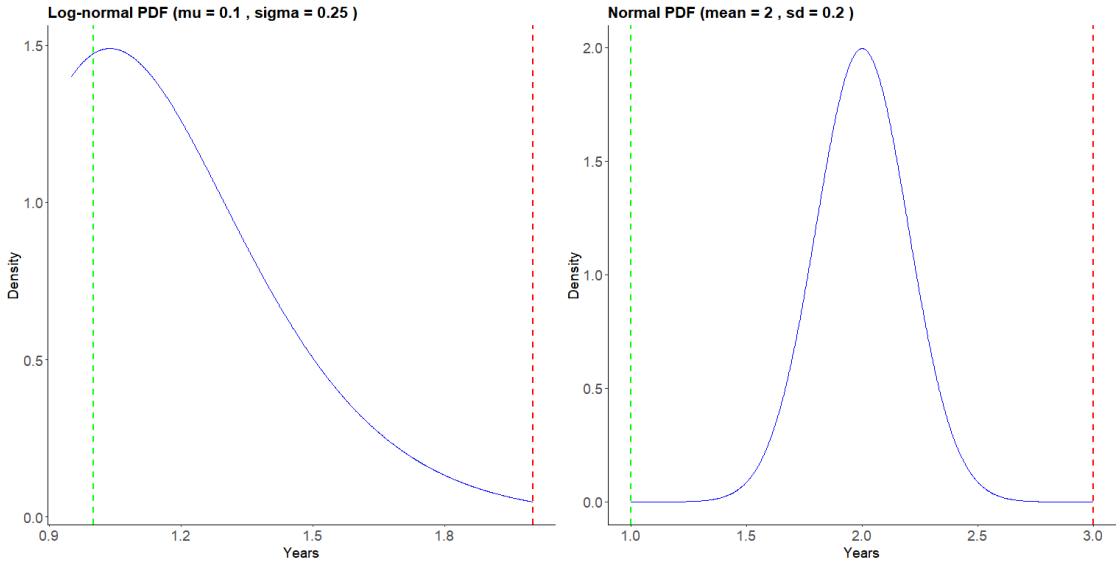

Figure3. Probability density of reproductive cycle different reproductive cycle scenarios.

Scenarios of demographic analysis

The primary outcome of the population demographic analysis is γ. The variability in γ is influenced by uncertainties in life-history parameters (Table 3). To assess the impact of these uncertainties, this study developed six scenarios to explore how variations in survival rates affect the estimates of γ:

Scenarios 1 and 2 (Table 4): These scenarios utilize growth parameters and age-at-maturity data from *Hall et al. (2012)*, differentiated by sex. Scenario 1 assumes a reproductive cycle of 1-2 years, with random values sampled from a lognormal distribution. Scenario 2 considers a reproductive cycle of 1-3 years, with values

randomly sampled from a normal distribution.

Scenarios 3 and 4 (Table 4): These scenarios apply growth parameters from *Varghese et al. (2016)*, which are not sex-specific. Scenario 3 assumes a reproductive cycle of 1-2 years, with random values sampled from a lognormal distribution. Scenario 4 considers a reproductive cycle of 1-3 years, with values randomly sampled from a normal distribution.

Scenarios 5 and 6 (Table 4): These scenarios utilize growth parameters from our study, based on longline observer data without differentiation between sexes. Scenario 5 assumes a reproductive cycle of 1-2 years, with values randomly sampled from a lognormal distribution. Scenario 6 considers a reproductive cycle of 1-3 years, with values randomly sampled from a normal distribution.

For each scenario, 10000 Monte Carlo simulations were conducted by sampling from the generated life-history parameters, including maturity-at-age, fecundity-at-age, maximum age, and age-at-maturity. The distributions of these parameters were used to estimate four demographic metrics: γ, R_0, G, and t_{x2}. These estimates were derived following the methods and definitions outlined in *Aires-da-Silva and Gallucci, (2007)*.

Table.3 Parameters Used for Different Scenarios.

Parameter	Value		Reference
	Female	Male	
L_∞	320.4(286.4—370.7)	277.3(252.9—311.0)	*(Hall et al., 2012)*
	309.8(Combine)		*(Varghese et al., 2016)*
	328.6(Combine)		*Estimated*
k	0.057(0.044—0.072)	0.079(0.062—0.101)	*(Hall et al., 2012)*
	0.1(Combine)		*(Varghese et al., 2016)*
	0.08(Combine)		*Estimated*
L_0	81.1(80.1—82.2)(Combine)		*(Hall et al., 2012)*
	66.3(Combine)		*(Varghese et al., 2016)*
	13.14(Combine)		*Estimated*
Longevity	25—35	25—35	*Estimated*
Weight(kg)-at-length	$W=2.045\times10^{-6}\times TL^{3.129}$	$W=1.580\times10^{-6}\times TL^{3.157}$	*(Hall et al., 2012)*
	$W = 4\times10^{-3}\times TL^{3.043}$(Combine)		*(Varghese et al., 2016)*
Age-at-maturity(yr)	14—16	13—14	*(Hall et al., 2012)*
	10.89	9.87	*(Varghese et al., 2016)*
	11.29	7.61	*Estimated*
Fecundity(litter size)	7.2(2—14)		*(Hall et al., 2012)*
Reproductive cycle	1—2		*Estimated*
	1—3		*Estimated*

Table.4 Growth parameters, age at maturity, reproductive cycle, and distribution of the reproductive cycle used in different scenarios.

Scenario	Growth parameter			Longevity	Weight(kg)-at-length	Age at maturity	Fecundity(litter size)	Reproductive cycle	Reproductive cycle distribution
	L_∞	k	L_0						
Scenario1	320.4(286.4—370.7)(Female) 277.3(252.9—311.0)(Male)	0.057(0.044—0.072)(Female) 0.079(0.062—0.101)(Male)	81.1(80.1—82.2)	25—35	$W=2.045\times10^{-6}\times TL^{3.129}$(Female) $W=1.580\times10^{-6}\times TL^{3.157}$(Male)	14—16(Female) 13—14(Male)	7.2(2—14)	1—2	Lognorrmal
Scenario2	320.4(286.4—370.7)(Female) 277.3(252.9—311.0)(Male)	0.057(0.044—0.072)(Female) 0.079(0.062—0.101)(Male)	81.1(80.1—82.2)	25—35	$W=2.045\times10^{-6}\times TL^{3.129}$(Female) $W=1.580\times10^{-6}\times TL^{3.157}$(Male)	14—16(Female) 13—14(Male)	7.2(2—14)	1—3	Normal
Scenario3	309.8(Combine)	0.1(Combine)	66.3	25—35	$W = 4\times10^{-3}\times TL^{3.043}$(Combine)	10.89(Female) 9.87(Male)	7.2(2—14)	1—2	Lognorrmal
Scenario4	309.8(Combine)	0.1(Combine)	66.3	25—35	$W = 4\times10^{-3}\times TL^{3.043}$(Combine)	10.89(Female) 9.87(Male)	7.2(2—14)	1—3	Normal
Scenario5	328.6(Combine)	0.08(Combine)	13.14	25—35	$W = 4\times10^{-3}\times TL^{3.043}$(Combine)	11.29(Female) 7.61(Male)	7.2(2—14)	1—2	Lognorrmal
Scenario6	328.6(Combine)	0.08(Combine)	13.14	25—35	$W = 4\times10^{-3}\times TL^{3.043}$(Combine)	11.29(Female) 7.61(Male)	7.2(2—14)	1—3	Normal

3 Results

Demographic analysis

Table 5 and Figure 4 presents demographic estimates of the γ across six different scenarios. Scenario 1 and Scenario 2 show relatively low mean intrinsic growth rates of 0.085 and 0.072, with 95% intervals that provide a moderate range of variability. In contrast, Scenario 3 and Scenario 4 exhibit higher mean growth rates of 0.136 and 0.120, respectively, and narrower 95% intervals, suggesting more stable population growth under these scenarios. Scenario 5 and Scenario 6 have intermediate mean values of 0.128 and 0.105, respectively, with a wide 95% interval, indicating substantial uncertainty.

Scenarios 3 and 4 show the shortest mean generation times, while Scenarios 1 and 2 have longer mean generation times, ranging from 13.2 to 15.9 years.

Table.5 Demographic estimates of different scenarios of the intrinsic rate of population increase (γ) and generation time (G).

Scenario	γ			G		
	Lower	Upper	Mean	Lower	Upper	Mean
Scenario1	0.058	0.110	0.085	16.2	18.6	17.4
Scenario2	0.047	0.095	0.072	16.3	18.6	17.4
Scenario3	0.112	0.158	0.136	12.1	13.0	12.5
Scenario4	0.099	0.138	0.120	12.2	13.1	12.7
Scenario5	0.070	0.175	0.128	10.1	11.4	10.6
Scenario6	0.053	0.149	0.105	10.2	11.4	10.7

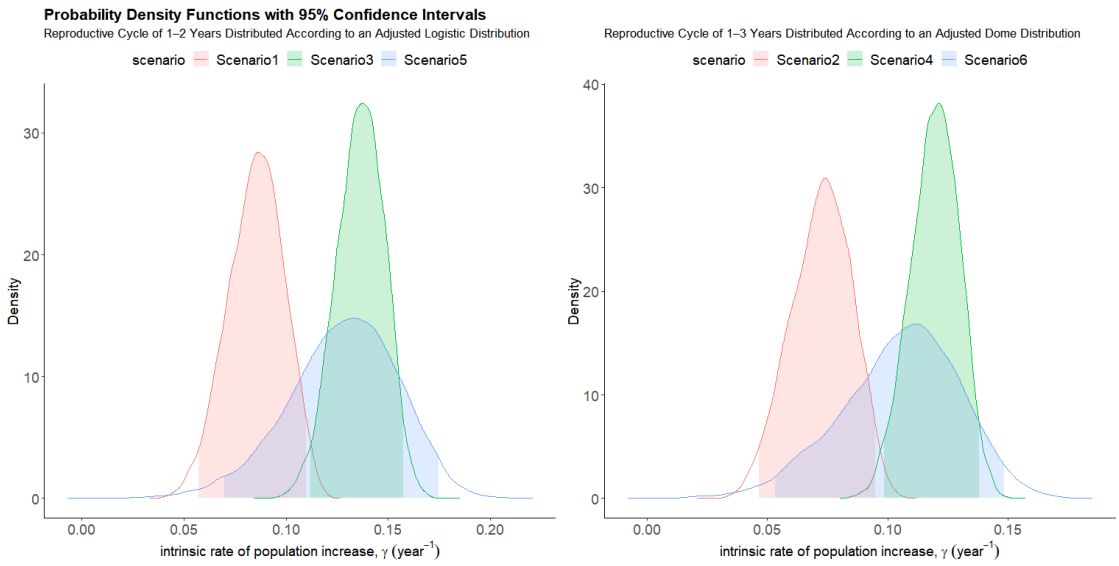

Figure4. Probability density of intrinsic rate of population increase of different reproductive cycle scenarios

Table 5 indicates that the mean generation time estimates range from 10.6 to 17.4 years across different scenarios. Table 6 indicates that the R_0 estimates across scenarios range from 1.80 to 7.25. Scenarios 3 show the highest mean values of 5.59, while Scenarios 2 and 6 have slightly lower mean values of 3.62 and 3.18, respectively. The estimated t_{x2} ranges from 3.96 to 14.9 years across different scenarios. Scenario 3 shows the shortest mean doubling time of 5.13 years, while Scenario 2 presents the longest mean doubling time of 9.92 years.

Table.6 Demographic estimates of different scenarios of net reproductive rate (R_0) and population doubling time (t_{x2}).

Scenario	R_0			t_{x2}		
	Lower	Upper	Mean	Lower	Upper	Mean
Scenario1	2.68	6.74	4.54	6.30	12.1	8.36
Scenario2	2.22	5.24	3.62	7.30	14.9	9.92
Scenario3	4.03	7.25	5.59	4.39	6.19	5.13
Scenario4	3.43	5.78	4.58	5.02	7.03	5.84
Scenario5	2.14	6.16	4.01	3.96	9.98	5.76
Scenario6	1.80	4.76	3.18	4.66	13.0	7.15

The h estimates across different scenarios, with mean values ranging from 0.291 to 0.506 (Table 7 and Figure 5). Scenario 3 exhibits the highest mean h of 0.506, indicating a steeper stock-recruitment relationship where recruitment is more sensitive to changes in spawning biomass. Conversely, Scenario 6 shows the lowest mean h of 0.291, reflecting a less pronounced sensitivity to changes in spawning biomass.

Table.7 Demographic estimates of different scenarios of h.

Scenario	h

	Lower	Upper	Mean
Scenario1	0.356	0.587	0.480
Scenario2	0.314	0.525	0.426
Scenario3	0.419	0.586	0.506
Scenario4	0.378	0.531	0.458
Scenario5	0.123	0.526	0.338
Scenario6	0.108	0.458	0.291

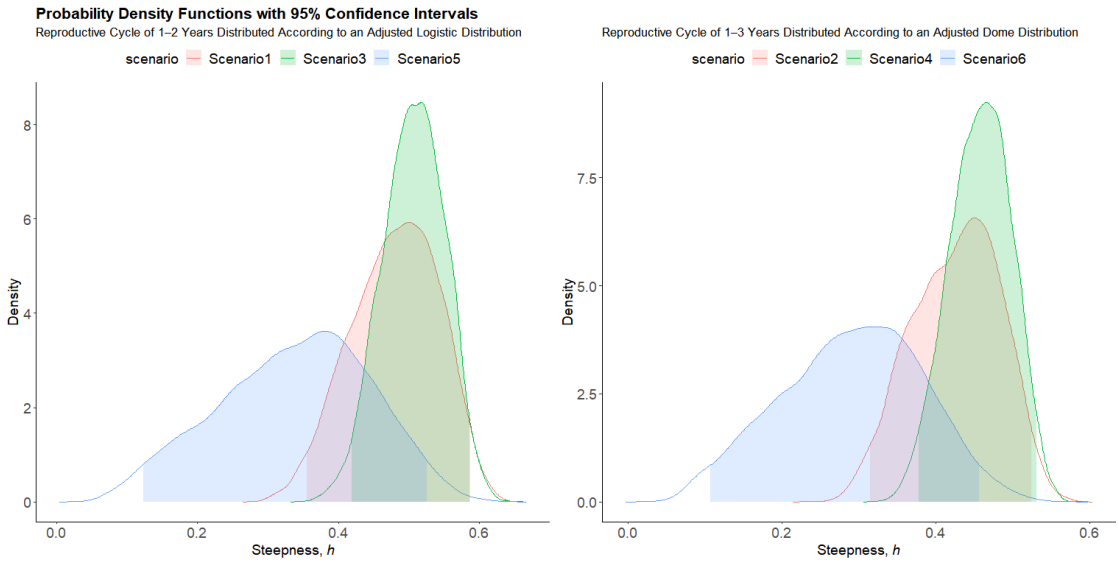

Figure5. Probability density of *h* of different reproductive cycle scenarios.

4 Discussion

4.1 Impact of Model Hypotheses and Parameter Uncertainty

In population demographic analysis, model assumptions and initial parameters significantly influence results. Sex-specific growth parameters, maximum length, and annual growth rates can lead to varying population dynamics estimates. Ignoring sex differences may result in inaccurate growth rates, age at maturity, and reproductive rates, affecting key parameters like intrinsic growth rate (γ) and generation time (G). Variations in these parameters shape individual growth and reproductive dynamics.

Assumptions about maximum age and reproductive rates are crucial, as longer lifespans lower growth rates and increase doubling times. Similarly, reproductive cycle length (e.g., 1-2 vs. 1-3 years) and choice of distribution models (lognormal vs. normal) impact fecundity estimates and population predictions. Methodological choices, such as probability distributions, further affect sensitivity to uncertainty. Thus, careful selection of both model settings and parameters is essential for improving precision and accuracy

in demographic analysis.

4.2 Management Implications for the Silky Shark in the Indian Ocean

Cramp et al. (2021) demonstrated that the prior range of the intrinsic growth rate (γ) significantly affects population assessments. *Urbina et al. (2018)* estimated a γ value of 0.062 for silky sharks using a low γ range, while Cramp's study provided ranges of 0.262-0.294 and 0.0454-0.0491 for low and extremely low γ levels, respectively. *Rice and Harley (2013)* found a γ of 0.102 for Pacific silky sharks, and *Clarke et al. (2015)* reported γ values of 0.078 for North Atlantic and 0.042 for South Atlantic silky sharks. The γ value estimated in this study aligns with these reasonable ranges.

Managing silky sharks in the Indian Ocean requires addressing the uncertainties highlighted in recent demographic analyses. Variability in γ, R_0, G, and t_{x2} across scenarios underscores the need for flexible management strategies. Scenarios with higher growth rates, like those using *Varghese et al. (2016)* parameters, suggest robust populations, while lower growth rates based on *Hall et al. (2012)* indicate vulnerability and slower recovery. Precautionary and adaptive strategies are vital to account for this uncertainty.

Accurate data collection is crucial, as discrepancies in initial parameters and model methods affect outcomes. Improved data quality and international cooperation are essential for managing migratory species like silky sharks, ensuring consistent data and coordinated conservation efforts to sustain their populations.

5 Reference

Aires-da-Silva, A. M., & Gallucci, V. F. (2007). Demographic and risk analyses applied to management and conservation of the blue shark (Prionace glauca) in the North Atlantic Ocean. *Marine Freshwater Research, 58*(6), 570-580.

Alejo-Plata, M. d. C., Ahumada-Sempoal, M. Á., Gómez-Márquez, J. L., & González-Acosta, A. (2016). Population structure and reproductive characteristics of the silky shark Carcharhinus falciformis (Müller & Henle, 1839)(Carcharhiniformes: Carcharhinidae) off the coast of Oaxaca, Mexico. *Latin American Journal of Aquatic Research, 44*(3), 513-524.

Anderson, R. C., Ahmed, H. J. F., Rome,, & Ministry of Fisheries, M., Maldives. (1993). *The shark fisheries of the Maldives*.pp.73

Bane, G. W. (1966). Observations on the silky shark, Carcharhinus falciformis, in the Gulf of Guinea. *Copeia, 1966*(2), 354-356.

Bonfil, R. (1997). Status of shark resources in the Southern Gulf of Mexico and Caribbean: implications for management. *Fisheries Research, 29*(2), 101-117.

Bonfil, R. (2008). The biology and ecology of the silky shark, Carcharhinus falciformis. *Sharks of the open ocean: biology, fisheries and conservation*, 114-127.

Branstetter, S. (1987). Age, growth and reproductive biology of the silky shark, Carcharhinus falciformis, and the scalloped hammerhead, Sphyrna lewini, from the northwestern Gulf of Mexico. *Environmental Biology of Fishes, 19*, 161-173.

Burns, E. S., Bradley, D., & Thomas, L. R. (2023). Global hotspots of shark interactions with industrial longline fisheries. *Frontiers in Marine Science, 9*, 1062447.

Caswell, H. (2006). *Matrix population models*. Sunderland. pp. 319-334

Compagno, L. J. (2001). *Sharks of the world: an annotated and illustrated catalogue of shark species known to date* (Vol. 2): Food & Agriculture Org. pp. 1-269.

Cortés, E. (2000). Life history patterns and correlations in sharks. *Reviews in Fisheries Science, 8*(4), 299-344.

Cortés, E. (2002). Incorporating uncertainty into demographic modeling: application to shark populations and their conservation. *Conservation biology, 16*(4), 1048-1062.

Cortés, E. (2008). Comparative life history and demography of pelagic sharks. *Sharks of the Open ocean: biology, fisheries, conservation, 2*, 309-322.

Filmalter, J. D., Capello, M., Deneubourg, J.-L., Cowley, P. D., & Dagorn, L. (2013). Looking behind the curtain: quantifying massive shark mortality in fish aggregating devices. *Frontiers in Ecology and the Environment, 11*(6), 291-296.

Galván-Tirado, C., Galvan-Magaña, F., & Ochoa-Báez, R. (2015). Reproductive biology of the silky shark Carcharhinus falciformis in the southern Mexican Pacific. *Journal of the Marine Biological Association of the United Kingdom, 95*(3), 561-567.

Geng, Z., Wang, Y., Kindong, R., Zhu, J., & Dai, X. (2021). Demographic and harvest analysis for blue shark (Prionace glauca) in the Indian Ocean. *Regional Studies in Marine Science, 41*, 101583.

Grant, M. I., Smart, J. J., White, W. T., Chin, A., Baje, L., & Simpfendorfer, C. A. (2018). Life history characteristics of the silky shark Carcharhinus falciformis from the central west Pacific. *Marine Freshwater Research, 69*(4), 562-573.

Hall, N., Bartron, C., White, W., Dharmadi, & Potter, I. (2012). Biology of the silky shark Carcharhinus falciformis (Carcharhinidae) in the eastern Indian Ocean, including an approach to estimating age when timing of parturition is not well defined. *Journal of Fish Biology, 80*(5), 1320-1341.

Hazin, F. H., Oliveira, P. G., & Macena, B. C. (2007). Aspects of the reproductive

biology of the silky shark, Carcharhinus falciformis (Nardo, 1827), in the vicinity of Archipelago of Saint Peter and Saint Paul, in the equatorial Atlantic Ocean. *Collective Volume of Scientific Papers: ICCAT, 60*, 648-651.

Hoyos-Padilla, E. M., Ceballos-Vázquez, B. P., & Galván-Magaña, F. (2012). Reproductive biology of the silky shark Carcharhinus falciformis (Chondrichthyes: Carcharhinidae) off the west coast of Baja California Sur, Mexico. *Aqua Int. J. Ichthyol, 18*, 15-24.

Joung, S.-J., Chen, C.-T., Lee, H.-H., & Liu, K.-M. (2008). Age, growth, and reproduction of silky sharks, Carcharhinus falciformis, in northeastern Taiwan waters. *Fisheries Research, 90*(1-3), 78-85.

Oshitani, S., Nakano, H., & Tanaka, S. (2003). Age and growth of the silky shark Carcharhinus falciformis from the Pacific Ocean. *Fisheries science, 69*(3), 456-464.

Sánchez‐de Ita, J., Quiñónez‐Velázquez, C., Galván‐Magaña, F., Bocanegra‐Castillo, N., & Félix‐Uraga, R. (2011). Age and growth of the silky shark Carcharhinus falciformis from the west coast of Baja California Sur, Mexico. *Journal of Applied Ichthyology, 27*(1), 20-24.

Simon, M., Fromentin, J.-M., Bonhommeau, S., Gaertner, D., Brodziak, J., & Etienne, M.-P. (2012). Effects of stochasticity in early life history on steepness and population growth rate estimates: An illustration on Atlantic bluefin tuna. *PloS one, 7*(10), e48583.

Smith, S. E., Au, D. W., & Show, C. (1998). Intrinsic rebound potentials of 26 species of Pacific sharks. *Marine Freshwater Research, 49*(7), 663-678.

Stevens, J. (1984). Life-history and ecology of sharks at Aldabra Atoll, Indian Ocean. *Proceedings of the Royal society of London. Series B. Biological sciences, 222*(1226), 79-106.

Stevens, J., & McLoughlin, K. (1991). Distribution, size and sex composition, reproductive biology and diet of sharks from northern Australia. *Marine Freshwater Research, 42*(2), 151-199.

Strasburg, D. W. (1958). Distribution, abundance, and habits of pelagic sharks in the central Pacific Ocean. *Fisheries, 1*, 2S.

Tsai, W.-P., Wang, Y.-J., & Yamaguchi, A. (2019). Demographic analyses of the data limited silky shark population in the Indian Ocean using a two-sex stochastic matrix framework. *Journal of Marine Science and Technology, 27*(1), 7.

Varghese, S. P., Gulati, D., Unnikrishnan, N., & Ayoob, A. (2016). Biological aspects of silky shark Carcharhinus falciformis in the eastern Arabian Sea. *Journal of the Marine Biological Association of the United Kingdom, 96*(7), 1437-1447.

Yokoi, H., Ijima, H., Ohshimo, S., & Yokawa, K. (2017). Impact of biology knowledge on the conservation and management of large pelagic sharks. *Scientific reports, 7*(1), 10619.